APPLIED ORGANOMETALLIC CHEMISTRY
Appl. Organometal. Chem. 2001; **15**: 407–413
DOI: 10.1002/aoc.162

Micro and sub-micro fabrication techniques for optically confined structures based on lithium fluoride†

R. M. Montereali,[1]* A. Mancini,[1] S. Martelli,[1] F. Menchini[1] and P. Picozzi[2]
[1]ENEA Centro Ricerche Frascati, PO Box 65, 00044 Frascati (RM), Italy
[2]INFM and Dip. Fisica, Università dell'Aquila, V Vetoio 10, 67010 Coppito (AQ), Italy

Lithium fluoride (LiF) films treated by low-energy electrons represent a very promising candidate for the realization of miniaturized broad band optical devices like active waveguides and microcavities. The main properties, in particular the refractive index, density, structure and microstructure, of polycrystalline LiF films grown by thermal evaporation on amorphous and crystalline substrates are discussed, together with their influence on colour centres formation induced by low-energy electron beam bombardment and on the choice of the main irradiation conditions. Copyright © 2001 John Wiley & Sons, Ltd.

Keywords: thin films; refractive index; electron beam lithography; LiF; colour centres; photoluminescence; integrated optics

INTRODUCTION

Integrated optics[1] covers a wide variety of device types, made using a large set of materials and techniques, and many of them are still not available commercially. Among them is lithium fluoride (LiF) treated by low-energy electrons,[2] which represents a very promising candidate for the realization of miniaturized broad band optical emitters, amplifiers and lasers operating in the visible spectral range.[3] Low-energy electron irradiation of LiF gives rise to the efficient formation of stable laser-active defects showing intense photoluminescence in the green and in the red spectral range at room temperature.[4] At the same time, the electron bombardment induces an increase in the real part of the refractive index of the irradiated area in the same wavelength interval where the emissions are located.[5]

Alkali halide (AH) crystals containing colour centres (CCs) have been extensively studied for the realization of optically pumped tuneable solid-state lasers.[6] Little attention, however, has so far been devoted to AH films and to their application in the development of innovative miniaturized coherent light sources, like active waveguides and microcavities. Broad band single-mode active channel waveguides have been realized for the first time at the surface of LiF single-crystals[7] and films[8] thermally evaporated on LiF bulk. The direct-writing lithographic process, which simultaneously induces the waveguiding structure and the photoluminescent CCs, looks like a promising method for designing a waveguiding structure on LiF. Nevertheless, this technique is strongly limited by the low refractive index of LiF, $\sim$1.39 at 633 nm, thus preventing it from being used for common substrate materials.

Recently, the fabrication of planar microcavities based on low-energy electron beam irradiated thin LiF films evaporated on Bragg reflectors has been achieved. A stack of films of alternatively high (H) and low (L) refractive index and proper thickness (the Bragg reflectors) constitutes such a structure. An LiF film containing photoluminescent CCs is interposed as the central spacer, and acts as light source. The engineering of the optical path travelled by the radiation inside such cavities permits the control of the emission properties of the active centres placed inside the spacer, e.g. an intensity and directionality enhancement for the light emitted along the normal to the layers at a chosen wavelength λ_{fab}. The good performances of these structures fundamentally rely on the exact control of the optical thickness for the LiF spacer

* Correspondence to: R. M. Montereali, ENEA Centro Ricerche Frascati, PO Box 65, 00044 Frascati (RM), Italy.
E-mail: montereali@frascati.enea.it
† Based on work presented at the 1st Workshop of COST 523: Nanomaterials, held 20–22 October 1999, at Frascati, Italy.

film. The film thickness, density and refractive index depend strictly on the deposition parameters, as well as on the nature of the substrate layers used. Also, the distribution of the emitting CCs inside the active layer is a crucial parameter: the low refractive index of LiF requires a maximum of CCs at the centre of the film to obtain a significant coupling with the forward-emitting mode of the structure.

The aim of the present contribution is an accurate analysis of the deposition parameters and their correlation with the refractive index, density, and microstructure of polycrystalline LiF films grown by thermal evaporation both on amorphous and crystalline substrates. Their influence on CCs formation induced by low-energy electron beam bombardment and the choice of the main coloration conditions, i.e. dose, depth of coloration and dose rate, will also be discussed.

EXPERIMENTAL

LiF films of thickness in the range from 0.3 to 3.8 μm were usually grown by thermal evaporation on different types of substrate maintained during deposition at a fixed temperature T_s between 30 and 370 °C. The LiF powder (Suprapur grade, by Merck) was heated at about 850 °C in a tantalum crucible placed in an evaporation chamber maintained at a pressure below 1 mPa. The evaporation rate was kept at $\sim$2 nm s^{-1}. The experimental details are described elsewhere.[9]

The LiF film thickness t was measured by a Tencor Alphastep profilometer.

Several LiF films deposited on fused silica substrates were optically characterized. The thickness t and the complex refractive index $n - ik$ of the film were the unknown quantities. The film complex refractive index was computed from transmittance and reflectance at quasi-normal incidence measurements performed with a Lambda-19 Perkin Elmer spectrophotometer.[10] The characterization was carried out over the wavelength range 350–2500 nm, in order to refine the thickness and to obtain information about the film model (homogeneous or inhomogeneous).[11]

The structural characterization of the samples was carried out by X-ray diffraction (XRD), used both in conventional Bragg–Brentano reflection mode and by performing texture analysis on the (111) and (200) LiF poles (Seifert PTS-3003 diffractometer).

The film surface morphology was investigated by atomic force microscopy (AFM) analysis with a Digital Nanoscope III using the tapping mode (TM) technique with silicon tips.

Low-energy electron beams (2–20 keV) were used to produce several kinds of CC at the surface of polycrystalline films. The irradiation was performed at room temperature (RT) in a mod. ISI ABT DS-130S scanning electron microscope (SEM) equipped with a lithography system. The beam current used was between 0.2 and 2 nA, directly measured with a Faraday cup placed on the sample holder. Typical irradiated areas were 3×3 mm^2, and several coloured stripes a few tens of micrometres wide and more than 10 mm long were defined.

The CCs formation was checked with several optical microscopy techniques, and by spectrally resolved absorption and photoluminescence measurements.[4] A Multiprobe 2001 confocal light scanning microscope (CLSM) system[12] from Molecular Dynamics equipped with an argon laser and a Nikon microscope was used to analyse several coloured stripes induced by electron beam lithography (EBL) on LiF films thermally evaporated on glass. The objective was immersed in oil and the nominal spatial resolution was 530 nm in depth and 270 nm in plane. An image can be reconstructed by scanning the focal volume through the sample and registering the signal as a function of spatial coordinates. This kind of system allows the specimen to be optically sectioned by scanning a series of planes, eliminating interference from adjacent, overlying and underlying fluorescence.[12] The samples were analysed by scanning for two channels simultaneously using the combination fluorescence + fluorescence with two argon excitation lines at 458 and 488 nm. In this configuration the emission signals were recorded simultaneously by two detectors with proper output filters to select the red and green emissions.

RESULTS AND DISCUSSION

LiF films grown on glass substrates

Profilometer measurements on LiF films showed a uniform film thickness with sharp edges and a smooth surface, which were almost replicas of the substrate surfaces. These features were also confirmed by the spectrophotometric measurements performed to compute the complex refractive

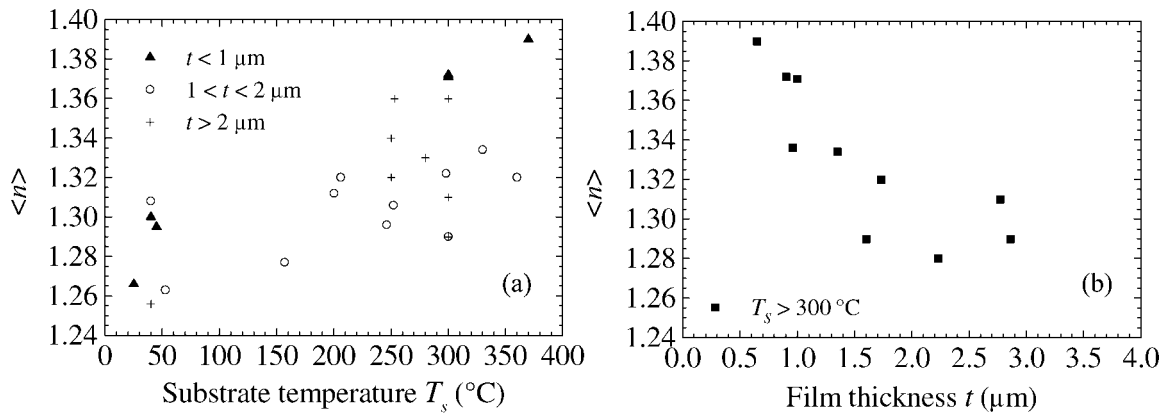

Figure 1 Mean refractive index of LiF films thermally evaporated on amorphous substrates as a function of substrate temperature T_s (a), and total film thickness t (b).

index of LiF films grown on amorphous transparent substrates. Significant differences in the optical properties of the deposited films were encountered depending on the growth conditions, especially T_s and t. In Fig. 1 the LiF films mean refractive indices are reported as a function of substrate temperature and film thickness. Up to 10% differences in the real part of the refractive index value could be obtained by simply varying these deposition parameters. In all the samples the extinction coefficient k was below 10^{-3}, and the real part n always lower than that of the bulk material. Raising the substrate temperature T_s induced an increase of the refractive index n, whereas n was generally lowered by increasing the film thickness, although in this latter case poor film adhesion and fracturing presented the major problem.

The refractive index is strongly related to the density of the deposited film, which is in turn dependent on the film structure. Higher substrate temperatures increase the mobility of the film molecules and thus favour the formation of more tightly packed microcrystals. As a matter of fact, the polycrystalline LiF films show different crystallite textures depending on T_s during evaporation.[9] It was observed[13] that, for LiF films of $t \geq 1$ μm, the higher the deposition temperature, the more the <100> LiF crystallographic direction approached the normal to the substrate plane, i.e. a close-packed stacking configuration with a corresponding increase in the film refractive index. An identical behaviour was observed in thin films (<1 μm) of LiF grown on glass substrates.

Figure 2 shows a typical (200) pole figure recorded on a thin LiF film deposited at low substrate temperature ($t = 0.55$ μm, $T_s = 40$ °C). The (200)-scattered intensity is well confined in a small region of the pole figure, attesting that the film possesses a nearly single-crystal grain texture. The intensity maximum is located 21 ° away from the origin, corresponding to the normal to the substrate plane. It can be deduced that the film is constituted by crystals all oriented with a <100> crystallographic direction forming an angle of about 21 °

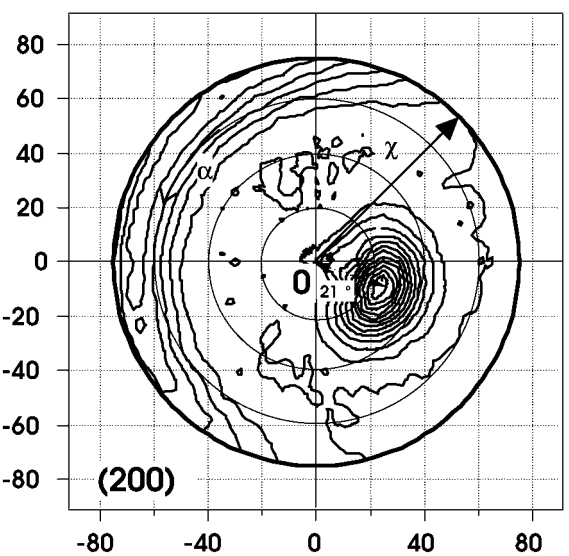

Figure 2 (200) pole figure recorded on an LiF film grown at low temperature on a glass substrate. Wavelength used: Cu Kα; tilt rotation $\chi \rightarrow 0$–75 °; azimuthal rotation $\alpha \rightarrow 0$–360 °; $\Delta\alpha,\chi = 5$ °; $2\theta = 45$ °.

Table 1 Densities ρ_f of LiF films having different refractive indices n, calculated by means of Eqn [2]

n	p	ρ_f (g cm^{-3})
1.27	0.69	1.82
1.30	0.77	2.02
1.33	0.84	2.23
1.36	0.92	2.43
1.3912 (bulk)	1	2.64

with the normal to the substrate plane. This angle is reduced to 10 ° for high substrate temperature films.

The relation between a dielectric film's refractive index and its density[14] can be estimated in a simplified way by considering the film as an aggregate of material 'grains' separated by air interstices. If we define the packing density $p = V_m/V_T$ as the fraction of total volume of the film occupied by the material, we find that inside the film a fraction (1-p) of the material (refractive index n_m) is replaced by air ($n_a \approx 1$). Thus, to a first approximation, the film index n is given by

$$n = (1 - p)n_a + pn_m \quad [1]$$

and

$$\rho_f = \rho_m p = \frac{n - 1}{n_m - 1} \quad [2]$$

By putting $n_m = 1.3912$ at 640 nm and RT and $\rho_m = 2.64$ g cm^{-3}, one obtains the values reported in Table 1 for the mean density of the as-grown LiF films on amorphous substrates.

LiF films grown on crystalline substrates

The comparison between a couple of thick LiF films grown at $T_s = 280$ °C in the same evaporation run over both a polished LiF single crystal and a glass substrate allows one to clarify better the relevance of the substrate nature on the properties of the deposited film. From the absence of an interference fringe pattern in the optical transmission spectrum of the first structure it could be deduced that the film refractive index was close to that of the bulk one (~1.39). This result can be ascribed to an epitaxial growth of the film on the LiF (100) single-crystal substrate, as confirmed by the appearance of just an intense (200) reflection in the XRD pattern and the perfect superposition of the substrate and film pole figures. Its thickness was 3.0 μm.

Conversely, the LiF film on glass had a refractive index of 1.34, which, according to Eqn [2], corresponds to a packing density $p \approx 0.87$. The thickness rises to 3.3 μm, which gives $p \approx 0.91$ if compared with the unity value of the above-mentioned thinner film grown on the bulk. The differences among these packing density values are negligible, when taking into account the simplified model adopted. As mentioned above, the sample on glass still presents a single-crystal texture, but with a <100> crystallographic tilt of 10 ° with respect to the normal to the substrate plane.

The AFM images of their surfaces are reported in Fig. 3a and b for the glass and LiF single crystal substrate, respectively. In the last case, the grain dimensions are quite irregular and the root-mean square (r.m.s.) of the surface roughness over an area of 4×4 μm^2 is about 47 nm. For the amorphous substrate the smoothness is improved and the roughness is lowered to 11 nm.

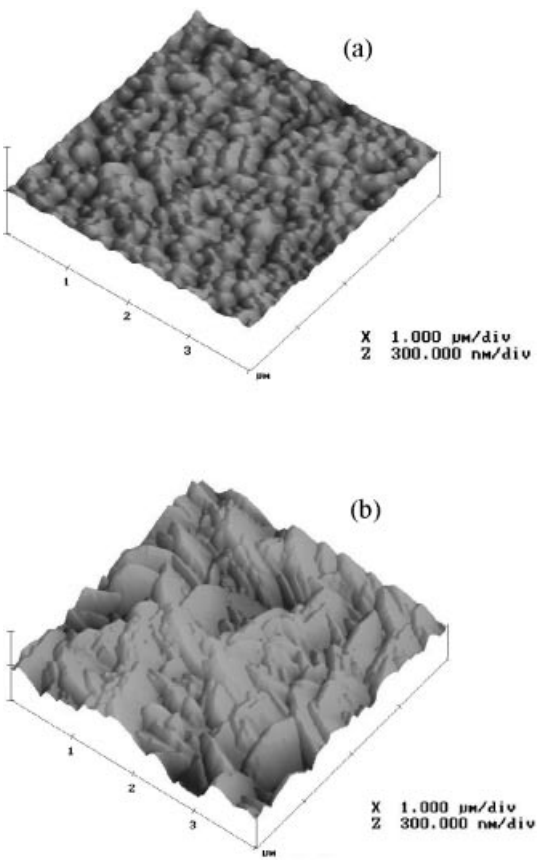

Figure 3 AFM images of two LiF films grown on a glass (a), and an LiF bulk substrate (b).

Electron irradiation of LiF films

Low energy (2–20 keV) electron beam irradiation produces several kinds of CCs located at the surface of LiF material, in the form of bulk and films. The electron penetration depth in AHs is related to the beam energy by the semi-empirical relation[15]

$$d = \frac{0.064}{\rho} E_e^{1.68} \quad [3]$$

where d (μm) is the maximum electron penetration depth, ρ (g cm^{-3}) is the compound density, and E_e (keV) is the electron beam energy. In LiF d ranges from 0.1 to 3.7 μm for electron energies between 2 and 20 keV. The rate of energy dissipation as a function of penetration for low-energy electrons in AHs has been investigated by several authors.[16] The electron energy distribution along the penetration depth is not a constant. Several computations showed that, for a given material, it is possible to construct a universal simplified curve of energy deposition *versus* penetration. This curve scales with d, and hence with energy; if d is the total range, then fd is the depth of maximum deposition rate,[17] where f is a material-dependent constant.

Monte Carlo simulation software[18] was used to determine the electron energy deposition along the depth and to verify the previous relation. In Fig. 4 the simulation results for LiF irradiated by 5 keV electrons are reported for the case of a bulk crystal and of a film of lower refractive index, taking into account the different densities of the two samples. The simulated maximum penetration depth is comparable to the values obtained from the semi-empirical relation in Eqn [3], and the depth of maximum energy deposition can also be estimated. An appreciable difference has been found in both the above parameters in the configurations investigated.

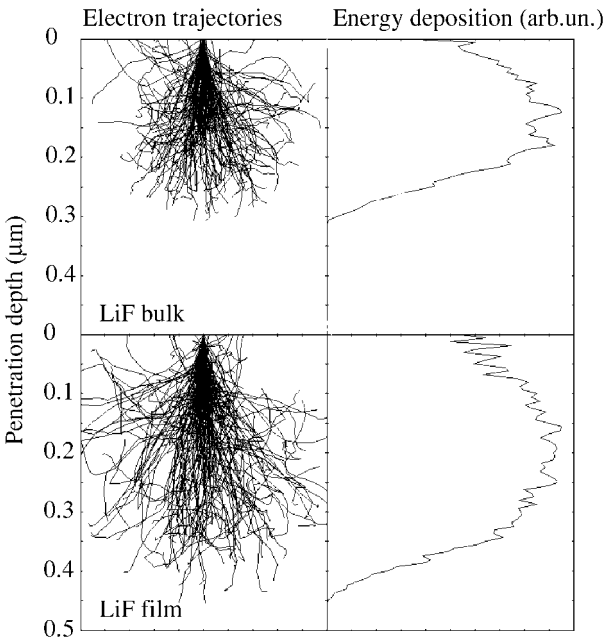

Figure 4 Monte Carlo simulations for an LiF bulk crystal (upper) and an LiF film of $n = 1.27$ (lower) irradiated by 5 keV electrons; on the left the electron trajectories are shown; on the right the electron energy deposition along the depth is plotted.

Confocal fluorescence scanning microscopy on coloured LiF films

The formation of the laser-active aggregate defects is associated with an apparent yellow coloration of the irradiated area, which can be recognized with a conventional optical microscope. By laser pumping the coloured samples in the active centres absorption bands, an intense visible photoluminescence is clearly observed by the naked eye. The high efficiencies of the green and red photoemissions from the laser-active F_3^+ and F_2 defects (two electrons bound to three and two anion vacancies respectively) under excitation in their almost overlapping absorption bands located around 450 nm allow one to employ a CLSM in fluorescence mode to reconstruct the laser-active defect distributions along the depth for a stripe induced by 12 keV electrons on a 2.6 μm thick polycrystalline LiF film thermally evaporated on glass at $T_s = 250$ °C.[19] Assuming the red fluorescence intensity to be proportional to the F_2 centre concentration, the F_2 defects' spatial profile along the depth can be reconstructed. The same can be done for the green emission signal, due to the F_3^+ centres. The results obtained are reported in Fig. 5, together with a Monte Carlo simulation of the 12 keV electron dose depth profile in LiF. The formation of the F_3^+ and F_2 aggregate defects appears mainly restricted to the electron penetration and is proportional to their energy depth profile, although some differences are found for depths greater than the estimated maximum penetration, depending also on the kinds of defect. The limited spatial resolution of the apparatus used in comparison with the maximum electron penetration at the selected energy does not give more detailed information about the sample investigated. Moreover, a high level of noise signal, probably ascribed to the polycrystalline nature of

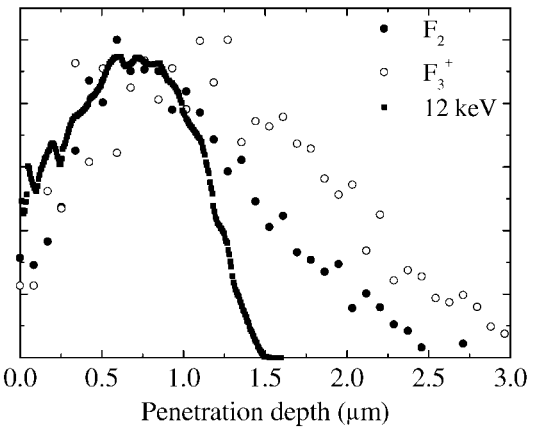

Figure 5 F_2 (●) and F_3^+ (○) fluorescence intensity spatial profile along the depth measured by confocal fluorescence microscopy on an LiF film irradiated by 12 keV electrons, and Monte Carlo simulation (■) of the energy depth profile in LiF for electrons of the same energy.

the sample being investigated, which causes a high scattering of the photoemitted light at the grain boundaries and at the interfaces, further affects the results obtained. The differences could be ascribed to the nature of the centres investigated, which are complex defects formed from the aggregation of primary ones,[20] as well as to a reduced density in the LiF film investigated, as shown in Fig. 4.

CONCLUSIONS

The use of versatile, well-assessed and low-cost fabrication techniques consisting of physical vapour deposition of LiF films on different kinds of substrate combined with an electron-beam direct-writing lithographic process allows the realization of optically confined active structures, like optical waveguides and microcavities. However, the development and optimization of the proper technological processes for their realization require the careful investigation of several properties, in particular the refractive index, density, structure and microstructure, of polycrystalline LiF films grown by thermal evaporation on amorphous and crystalline substrates. Their influence on the main features of CCs formation induced by a low-energy electron beam has been discussed. In particular, the electron energy depth distribution has been investigated by using Monte Carlo simulation software and from experimental measurements obtained for the first time in this kind of material by a CLSM system.

Further experiments are under way on stripe-like regions induced by EBL at higher energies on thicker films grown on different types of substrate in order to clarify better the interaction between the insulating material investigated and the ionizing radiations used. However, the influence of the polycrystalline structure and morphology of the LiF films on the formation, aggregation and stabilization of different kinds of aggregate defect still requires a deep investigation of their properties and interactions.

Acknowledgements The authors would like to acknowledge the valuable discussions with Dr G. Baldacchini and Professor E. Burattini. They are indebted to A. Pace for his precious technical contribution in the film preparation, to A. Grilli and A. Raco for skillful assistance in the electron irradiation and to T. Lepidi for AFM measurements. Many thanks are due to D. C. Joy and E. Napchan for elaborating and providing the Monte Carlo simulation software.

REFERENCES

1. Tamir T. *Integrated Optics*. Springer Verlag: Berlin; 1977.
2. Montereali RM, Martelli S, Righini GC, Pelli S, Afonso CN, Perea A, Barbier D, Bruno P. In *9th CIMTEC–World Forum on New Materials, Symposium X—Innovative Light Emitting Materials*, Vincenzini P, Righini GC (eds.). Techna s.r.l.: 1999; 321.
3. Montereali RM. *Rad. Eff. Def. Solids* 1999; **149**: 189.
4. Montereali RM, Baldacchini G, Scavarda do Carmo LC. *Thin Solid Films* 1991; **201**: 106.
5. Montecchi M, Nichelatti E, Mancini A, Montereali RM. *J. Appl. Phys.* 1999; **86**: 3745.
6. Mollenauer LF. *Tunable Lasers*. Springer Verlag: Berlin; 1987.
7. Montereali RM, Mancini A, Righini GC, Pelli S. *Opt. Commun.* 1998; **153**: 223.
8. Fornarini L, Martelli S, Mancini A, Righini GC, Pelli S. In *Proceedings of the 9th European Conference on Integrated Optics*, ECIO'99, Turin, Italy, 1999; 343.
9. Montereali RM, Baldacchini G, Martelli S, Scavarda do Carmo LC. *Thin Solid Films* 1991; **196**: 75.
10. Macleod HA. *Thin Film Optical Filters*. Macmillan Publishing Company: New York; 1986.
11. Montecchi M, Masetti E, Emiliani G. *Pure Appl. Opt.* 1995; **4**: 15.
12. Pawley JB (ed.). *Handbook of Biological Confocal Microscopy*. Plenum Press: New York; 1990.
13. Di Nunzio PE, Fornarini L, Martelli S, Montereali RM. *Phys. Status Solidi A*, 1997; **164**: 747.
14. Pulker HK. *Appl. Opt.* 1979; **18**: 1969.

15. Ortiz C, Macfarlane RM, Shelby RM, Lenth W, Bjorklund GC. *Appl. Phys.* 1981; **25**: 87.
16. Seifert N, Ye H, Tolk N, Husinsky W, Betz G. *Nucl. Instrum. Methods B* 1994; **84**: 77 and references cited therein.
17. Jammal YA, Pooley D, Townsend PD. *J. Phys. C: Solid State Phys.* 1973; **6**: 247.
18. Joy DC. *J. Microsc.* 1987; **147**: 51.
19. Montereali RM, Bigotta S, Piccinini M, Giammatteo M, Picozzi P, Santucci S. *Nucl. Instrum. Methods B* 2000; **764**: 166.
20. Baldacchini G, Cremona M, d'Auria G, Martelli S, Montereali RM, Montecchi M, Burattini E, Grilli A, Raco A. *Nucl. Instrum. Methods B* 1996; **116**: 447.

